

M.A. Admiraal · W.P. Medendorp · C.C.A.M. Gielen

Three-dimensional head and upper arm orientations during kinematically redundant movements and at rest

Received: 23 February 2001 / Accepted: 4 September 2001 / Published online: 30 November 2001
© Springer-Verlag 2001

Abstract The three rotational degrees of freedom of the head and the upper arm exceed the number needed in a two-dimensional (2-D) facing or pointing task, respectively. Previous studies reported a reduction of the number of degrees of freedom from three to two, with one degree of freedom being a unique function of the other two (Donders' law). This study investigated whether three-dimensional (3-D) orientations of the head and arm are the same at rest and during movement for corresponding pointing or facing directions. Two separate experiments were performed: one focused on head orientations, the other focused on upper arm orientations. We instructed subjects to direct the nose or to point the extended arm in the direction of targets, which appeared in a quasi-random order at 2-s intervals. The head and upper arm orientations at rest were described by a 2-D surface with a scatter less than 3 or 4°, respectively. Both for the arm and the head, orientations started and ended near the 2-D surface, but for a number of the target pairs, the orientations deviated from those predicted by the 2-D surface during movement in a way that was consistent and reproducible for movements between each target pair. For upper arm movements, we often found that deviations of arm orientations from the 2-D surface increased with increasing movement velocity. Such a positive correlation between deviation and movement velocity was not found for head movements. These results clearly indicate violations of Donders' law during movement and argue against several models for movement control found in the literature.

Keywords Motor control · Movement · Donders' law

Introduction

A pointing direction of the fully extended arm can be obtained in many different orientations of the upper arm with the rotation of the upper arm along its long axis as a redundant degree of freedom. In other words, straight-arm pointing determines only two of the three rotational degrees of freedom of the shoulder. Despite this kinematic redundancy, several studies have reported consistent and reproducible three-dimensional (3-D) upper arm orientations during straight-arm pointing movements (e.g. Straumann et al. 1991; Theeuwens et al. 1993; Medendorp et al. 2000). Similarly, the three rotational degrees of freedom of the head exceed the number necessary to specify the head's facing direction. Yet various studies have shown that 3-D head orientation is uniquely determined by two-dimensional (2-D) facing direction (Glenn and Vilis 1992; Radau et al. 1994; Medendorp et al. 1999). These findings reflect a reduction of the number of rotational degrees of freedom, an observation known as Donders' law.

Donders' law is expressed by the fact that the rotation vectors, which describe the orientation of the upper arm or head as a rotation relative to some reference orientation, are constrained to a 2-D surface (Glenn and Vilis 1992; Hore et al. 1992; Miller et al. 1992). A strict interpretation of Donders' law requires that this surface, which appears to be curved for the upper arm and the head, should equally well describe orientations during movements and orientations at rest (i.e. orientations before and after a movement). Although this has been implicitly assumed in many studies (e.g. Straumann et al. 1991; Miller et al. 1992; Theeuwens et al. 1993), the literature presents some contradictory observations on this issue. Hore et al. (1992) tested orientations of the hand during movement and at rest and did not find any differences. However, Crawford et al. (1999) reported that head movements of monkeys made transient but dramatic departures from the 2-D surface, taking the shortest path between two eccentric fixation points on the surface. Similar observations were found in humans for fast back-and-forth head movements (Tweed and Vilis 1992).

M.A. Admiraal (✉) · W.P. Medendorp · C.C.A.M. Gielen
Department Medical Physics and Biophysics,
University of Nijmegen, Geert Grooteplein 21,
6525 EZ Nijmegen, the Netherlands
e-mail: marjana@mbfys.kun.nl
Tel.: +31-24-3614244, Fax: +31-24-3541435

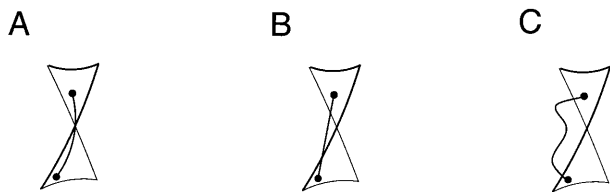


Fig. 1A–C The implications for movement strategies in rotation vector space. The 2-D surface is the same in each panel. *Solid dots* indicate the initial and final positions. **A** Moving along the 2-D surface. When orientations during movement obey Donders' law, the angular rotation axis cannot be a fixed rotation axis but changes in time. **B** Fixed-axis rotation between two orientations that obey Donders' law. The movement path in rotation vector space is shorter than in **A**. **C** Moving along a variable axis. When Donders' law is violated during movement with angular rotation vectors which are not fixed, many different trajectories from initial to final orientation are possible

Until now, a systematic analysis of the validity of Donders' law during upper arm or head *movements* has not been done. Elaborating on previous literature, which agrees on the observation that orientations at rest can be described by a 2-D surface, the present study specifically examines whether orientations during movements are constrained to the same 2-D surface.

The notion that orientations at rest can be described by a 2-D surface is compatible with other studies, which have suggested that the final arm orientation after a reaching movement is planned in advance and is used as a control variable by the central nervous system (CNS) (see e.g. Flanders et al. 1992; Rosenbaum et al. 1995; Gréa et al. 2000). In this context, the effect of movement velocity could be important. The presumption of this study, i.e. the validity of Donders' law for head and upper arm orientations at rest, implies that movement velocity will not affect the orientations at the end of the movement, which is in agreement with the results of Nishikawa et al. (1999). However, during the movement the effect of movement velocity on the adopted orientations remains to be seen. Low velocity movements can be regarded as a sequence of orientations at rest, corresponding to a trajectory along the surface. If movement velocity increases, trajectory control might be less tight and deviations from the surface might occur. If this holds true, then various trajectories can be hypothesized to move the arm or head from the initial to the final orientation, as shown in Fig. 1.

When Donders' law applies at all times, irrespective of movement velocity, then all orientations during a movement are constrained to the same curved surface, which describes the orientations at rest (Fig. 1A). This requires a non-fixed rotation axis in the shoulder or head and implies that the motor program to move the arm along a complex trajectory in the curved 2-D surface should be rather complicated. The second hypothesis is that the motor program brings the arm or head with a single, fixed-axis rotation from the initial to the final orientation, as shown in Fig. 1B (see also Crawford et al. 1999). In that case orientations during movement lie on a

straight line between the rotation vectors which specify initial and final orientation, independent of movement velocity. Such a movement clearly violates Donders' law, since in this case the orientations during the movement do not coincide with the curved surface describing orientations at rest. As to the third hypothesis, illustrated in Fig. 1C, the CNS only specifies initial and final orientations but does not take into account the complex biomechanical properties of the extended arm or the head, thus avoiding complicated computations associated with multi-joint movements. In such a strategy, movement velocity might influence the orientations during the movement. The first two hypotheses (Figs. 1A, B) imply that orientation during a movement is carefully controlled by the CNS throughout the movement, whereas the latter (Fig. 1C) does not necessarily require a strict control of orientations during a movement.

Summarizing, the aim of this study is to investigate whether orientations of the upper arm and head are the same at rest and during movement for equal pointing and facing directions, respectively, and how any differences might be influenced by movement velocity. The answer to this question provides new data for comparison with predictions from various models in the literature about motor control.

Materials and methods

This study investigated 3-D orientations of the upper arm and head in two separate experiments. The experiments were approved by the ethics committee of the University Medical Center. Five adult subjects (aged 26–47 years) participated in the experiments; all gave their informed consent. None of the subjects had any known history of neurological or musculo-skeletal disorders. Two subjects (SG and PM) were familiar with the purpose of the experiments. The results of these subjects were not different from those of the other subjects. All subjects were right-handed and pointing movements were made with the right arm.

Experimental setup

The subject sat with the trunk fixated to the chair such that the shoulder and head were free to rotate in all directions. In both the arm and the head experiment, the subject was positioned such that the central target (target 5 in Fig. 2) was near the centre of the mechanical range of the upper arm or head, respectively.

Visual stimuli generated by a personal computer were projected by a LCD projector (Philips Proscreen 4750) on a translucent screen. For the arm movement experiment, the screen was placed at a distance of 90 cm from the subject's shoulder. For the head movement experiment, the distance between the screen and the subject's eyes was 80 cm. The visual scene covered an area of 120×96 cm, which consisted of a checkerboard pattern with 8×8 alternating black and yellow rectangles (15×12 cm each) and a bright yellow, circular target with a diameter of 1.5 cm that appeared on top of the checkerboard pattern. Targets could appear at nine locations, situated on a rectangular or square grid for the arm and head, respectively (see Fig. 2). Zero-elevation and zero-azimuth were defined as the elevation and azimuth when the subject was pointing or facing straight ahead. With these definitions, the workspace of the shoulder ranged from 0° to +67° in azimuth, and from –26.5° to +26.5° in elevation. The workspace for the head ranged from –25° to +25° for both azimuth and elevation.

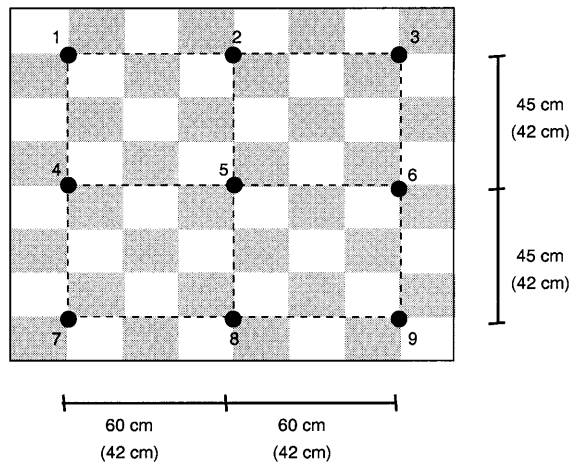


Fig. 2 Schematic overview of the nine targets on a checkerboard background. Movement paths included in the evaluation are indicated by *dotted lines*. Distance between targets is indicated for the arm (and for the head in parentheses)

The position and orientation of the upper arm and head were measured with an Optotrak 3020 system (Northern Digital, Ontario, Canada), which measures the 3-D position of infrared-light-emitting-diodes (IREDs) with a resolution better than 0.2 mm within a range of about 1.5 m³. The Optotrak system was mounted on the ceiling above the subject at a distance of approximately 2.5 m behind the seated subject, tilted downward at an angle of 30° relative to the ceiling. In both experiments, positions of IREDs were measured at a sampling frequency of 100 Hz.

To measure the orientation of the upper arm, a cross with IREDs on each of the four tips was attached to the upper arm, about 2 cm proximal to the elbow. The length of each arm of the cross was 2.5 cm. The position of the cross was adjusted such that the Optotrak system could always measure the position of at least three IREDs during all movements. We were able to determine orientations for the upper arm with an accuracy better than 0.3° in all directions.

To determine head orientations, subjects were wearing a helmet with four IREDs mounted on top and two IREDs on the back (see Medendorp et al. 1998). The weight of the helmet, which was firmly fixed to the head, was less than 0.25 kg. At all times during the experiment, at least three IREDs were visible for the Optotrak. Head orientations could be determined with an accuracy better than 0.2° in all directions (see Medendorp et al. 1998; Veldpaus et al. 1988).

Experimental protocols

Arm

At the start of each sequence of movements, subjects pointed to the central target to define a reference orientation for the arm. Next, the subjects had to point toward new targets that appeared in quasi-random order at the nine target positions at 2-s intervals. Six combinations of start and end targets occurred more frequently than others (target pairs 1–3, 4–6, 7–9, 1–7, 2–8 and 3–9; see Fig. 2). These target pairs resulted in either vertical or horizontal movements at different azimuth or elevation angles. Since movements were made in both directions, 12 different movements were analysed. Each pair of targets occurred at least 32 times during the complete set of movements, 16 times for each movement direction. In order to prevent fatigue, subjects were tested in 16 blocks with 20 movements each. Each block lasted about 40 s and was followed by a brief rest period. Subjects were instructed to point with the fully extended arm from target to target with a single aiming movement.

Instruction for movement velocity, indicated by ‘normal’, ‘low’ or ‘high’, was given at the beginning of each block of 20 movements, which resulted in a range of velocities from about 50 to 200°/s. Movements that were not completed within the 2-s interval of target presentation, and movements that were initiated in a wrong direction, were discarded from further analysis.

Head

Subjects were instructed to point their nose toward the targets that appeared at an interval of 2 s. As with the arm, a wide range of movement velocities was tested, ranging from about 100 to 300°/s. All subjects made 320 head movements, divided into 16 blocks with 20 movements each. Movements were discarded from further analysis when a new target appeared before the movement to the previous target was completed. The same target pairs as described for the arm were used for the head measurements: the six pairs of initial and final positions all occurred at least 32 times; 16 times for each movement direction.

Data analysis

IRED data initially were represented in a coordinate system related to the Optotrak system. For evaluation purposes, the data were transformed into a right-handed coordinate system, with the x-axis defined along the pointing or facing direction of the reference position, the z-axis vertically pointing upwards and the y-axis perpendicular to both.

The orientation of the upper arm or head was described by a rotation vector, which rotates a particular reference position into the current position. This rotation vector is defined as $\vec{r} = \tan(\theta/2) \cdot \vec{n}$, where \vec{n} represents the direction of the rotation axis in 3-D, and θ the angle of the rotation around this axis (see Hausteil 1989).

Beginning and end of a movement were determined on the basis of an angular velocity criterion (threshold: 10°/s). This threshold enabled us to investigate almost the complete range of orientations along the movement trajectory. Accordingly, static orientations are defined as those orientations of the upper arm or head corresponding to angular velocities below 10°/s. Next, we fitted a second-order function to the static rotation vector data, given by:

$$r_x = a + br_y + cr_z + dr_y^2 + er_yr_z + fr_z^2 \quad (1)$$

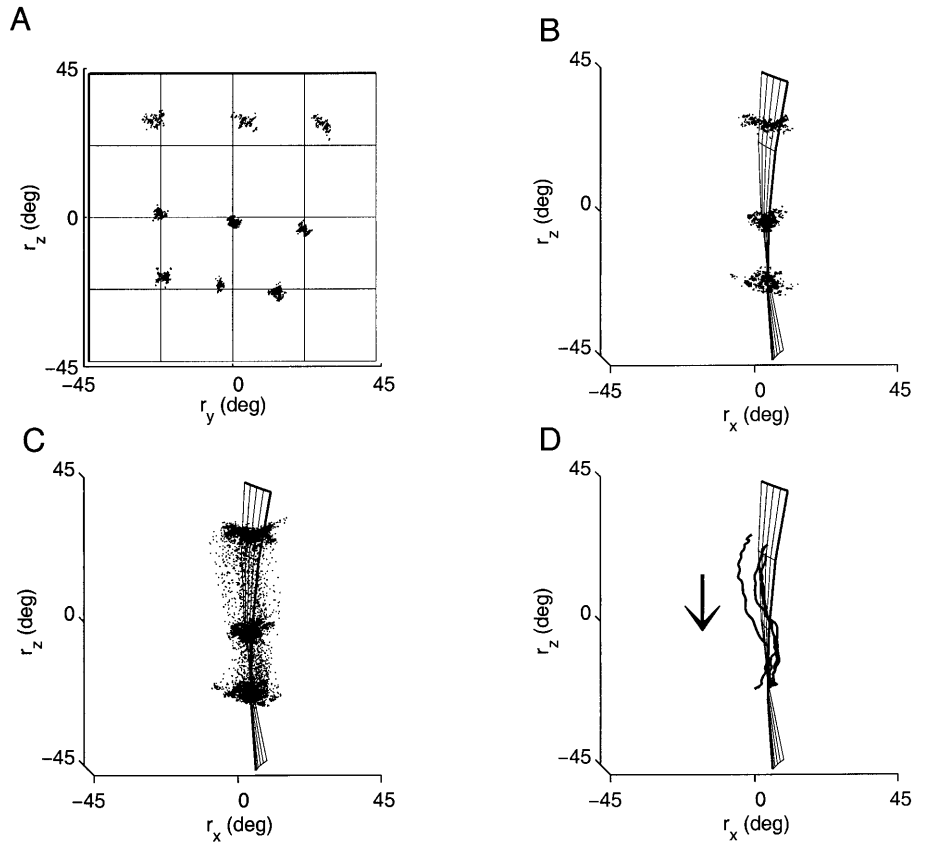
where r_x , r_y and r_z represent the torsional, vertical and horizontal components of the rotation vector \vec{r} , respectively. This description represents a 2-D surface in a 3-D rotation vector space. The scatter of the data relative to the fitted surface is described by the standard deviation of the distances in torsional direction of the rotation vectors towards the fitted surface (see Glenn and Vilis 1992; Hore et al. 1992; Theeuwes et al. 1993; Gielen et al. 1997; Medendorp et al. 1999).

Evaluating deviations from the surface

Since we were interested in the spatial aspects (i.e. orientation) of the upper arm and head during a movement rather than in the temporal aspects, each trajectory was spatially resampled onto 250 equidistant sample points. Consequently, the (constant) distance between two sample points depended on the total length of the trajectory.

We evaluated the 3-D trajectory of orientations of the head and upper arm during a movement, and compared it to a trajectory along the surface, referred to as ‘predicted trajectory’. Since many different trajectories are available to move from the starting position to the final position along a curved surface, one trajectory over the surface had to be selected. We compared the measured trajectory with the trajectory over the surface described by the projection of this measured trajectory on the curved surface in torsional direction. This trajectory represents positions with the

Fig. 3A–D Rotation vectors and 2-D surface for the static (A, B) and movement (C, D) orientations of the arm. **A** The projections on the plane of the horizontal and vertical rotational components. *Dots* indicate the rotation vectors of the all orientations reached with a velocity $<10^\circ/\text{s}$. The nine clusters in **A** correspond to pointing to the nine targets. **B** A quasi 3-D view on the 2-D surface fitted to the static data. **C** The *dots* represent rotation vectors of orientations both at rest and during movements with self-paced velocity. One of every three measured orientations is shown. **D** The four *lines* represent data of arm orientations for four movements from target 1 to target 3



same amounts of elevation and azimuth as the measured orientations, but possibly with a different amount of torsion. Should the measured trajectory lie in the surface, then the measured trajectory and the predicted trajectory fully coincide.

As a measure of the correspondence of torsion of the trajectories as a function of azimuth and elevation for movements with the same start and end position, we calculated the correlation coefficient between the trajectory – spatially resampled – in rotation vector space for a movement and the mean of the trajectories of the other movements with the same start and end position. We performed this calculation for the five fastest movements for each subject and each pair of targets. For each of these five movements, we also calculated the correlation coefficient between the trajectory and the predicted trajectory along the surface. When movements reveal systematic deviations of torsion relative to the predicted trajectory, the correlation of a movement trajectory with the mean of the other trajectories should be larger than the correlation with the predicted trajectory. We compared the mean correlation coefficient between the trajectories relative to each other with the mean correlation coefficient for the trajectories with the predicted trajectory. Differences in mean correlation coefficients were evaluated by means of a *t*-test.

We used a different analysis to test the effect of movement velocity on the orientations during movements. Orientations during movements sometimes appeared to have a small constant bias in torsional direction, corresponding to the torsional bias at the onset of the movement. For a good comparison of the measured trajectories for different movement velocities, we have shifted each measured trajectory in torsional direction such that the initial and final orientations lie as close as possible to the fitted surface. This shift was small, typically 1 to 3° . This procedure was applied only for the data on effects of velocity and velocity-dependent deviations. Deviations from the surface were calculated as the distance between the shifted measured trajectory and the predicted trajectory. Since all trajectories were spatially resampled into 250 equidistant points, this corresponds to a summation of the distances of all 250

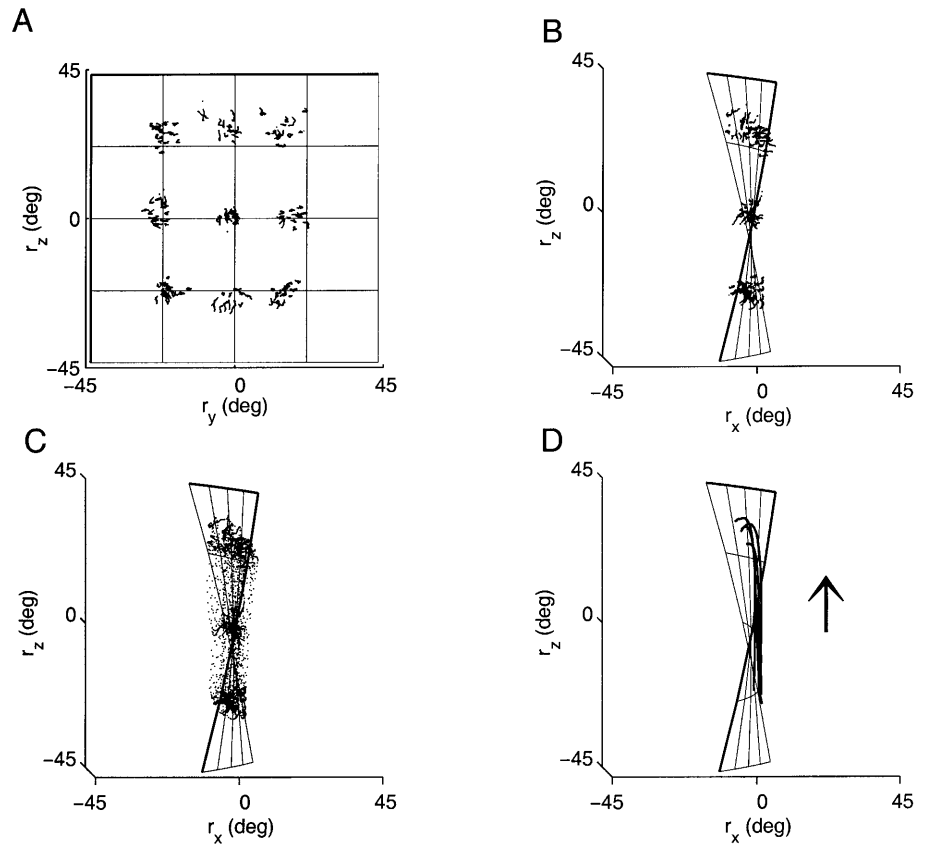
measured data points relative to the predicted data in the 2-D surface. In order to test whether movement velocity influences the amount of deviation relative to the surface, we calculated the correlation coefficient between peak velocity and deviation from the surface, for each pair of targets.

Results

In this study we tested whether orientations of the upper arm and the head are the same during movement and during fixation at corresponding targets. Since the results for the head and upper arm reveal several similarities, they will be discussed simultaneously.

Figure 3 shows, for subject SG, the rotation vectors representing the orientations of the upper arm in the arm experiment. The upper panels show the rotation vectors representing the static orientations, i.e. orientations with angular velocities below $10^\circ/\text{s}$ (see Materials and methods). A 2-D surface was fitted to the data sets using Eq. 1. Figure 3A provides a frontal view on the static data and the 2-D surface. Figure 3B provides a side view on the same surface in 3-D space, such that the scatter of the data relative to the curved surface can be observed as clearly as possible. For the upper arm orientations depicted in Fig. 3A, B, the standard deviation of the data relative to the surface is 3.1° . For all subjects, the standard deviation varied between 3.1 and 4.6° (mean 3.8° , SD 0.6°). Figure 3 shows that the best fitting surface to the arm data is not a flat plane, but a surface with a curvature and

Fig. 4A–D Rotation vectors and 2-D surface for the static (**A, B**) and movement (**C, D**) orientations of the head. **A** The projections on the plane of the horizontal and vertical rotational components. *Dots* indicate the rotation vectors of the orientations reached with a velocity $<10^\circ/\text{s}$. The nine clusters in **A** correspond to facing the nine targets. **B** A quasi 3-D view on the 2-D surface fitted to the static data. **C** *Dots* represent rotation vectors of orientations both at rest and during movements with self-paced velocity. One out of every three measured orientations is shown. **D** The four *lines* represent data of head orientations for five movements from target 1 to target 3



a twist (coefficients d , e and f in Eq. 1). For all subjects, the surfaces are slightly curved and twisted, although considerable inter-subject variability occurs in the amount of curvature and twist. For all subjects, the mean twist coefficient (coefficient e in Eq. 1) was -0.03 (SD 0.12 , range -0.20 to 0.11). The values of the coefficients d and f , which indicate the curvature of the surface, are of the same magnitude as that of the twist coefficient e [mean values -0.01 (SD 0.18) and 0.15 (SD 0.19) for coefficients d and f , respectively].

Figure 3C shows the same data as those of Figs. 3A, B, complemented by the rotation vectors for orientations during movements that were made at self-paced velocities. For the sake of clarity we plotted one of every three sampled data points during the movement, since showing all data points would create a dense cluster of points, obscuring any differences between rotation vectors for the arm at rest and during movement. At first glance, the scatter of the movement data relative to the surface does not appear to differ much from that of the data at rest relative to the same surface. A quantitative analysis reveals that for this subject the scatter is slightly smaller for the static data than for the movement data (3.1° vs 3.9°). This was found for all subjects [mean 3.8° (SD 0.6) vs 4.2° (SD 0.5) for static and movement data, respectively]. A t -test revealed that this difference in scatter between the data at rest and the movement data was significant ($t=3.42$, $P<0.05$).

A more detailed analysis demonstrates that the scatter of the rotation vectors for arm movement data relative to

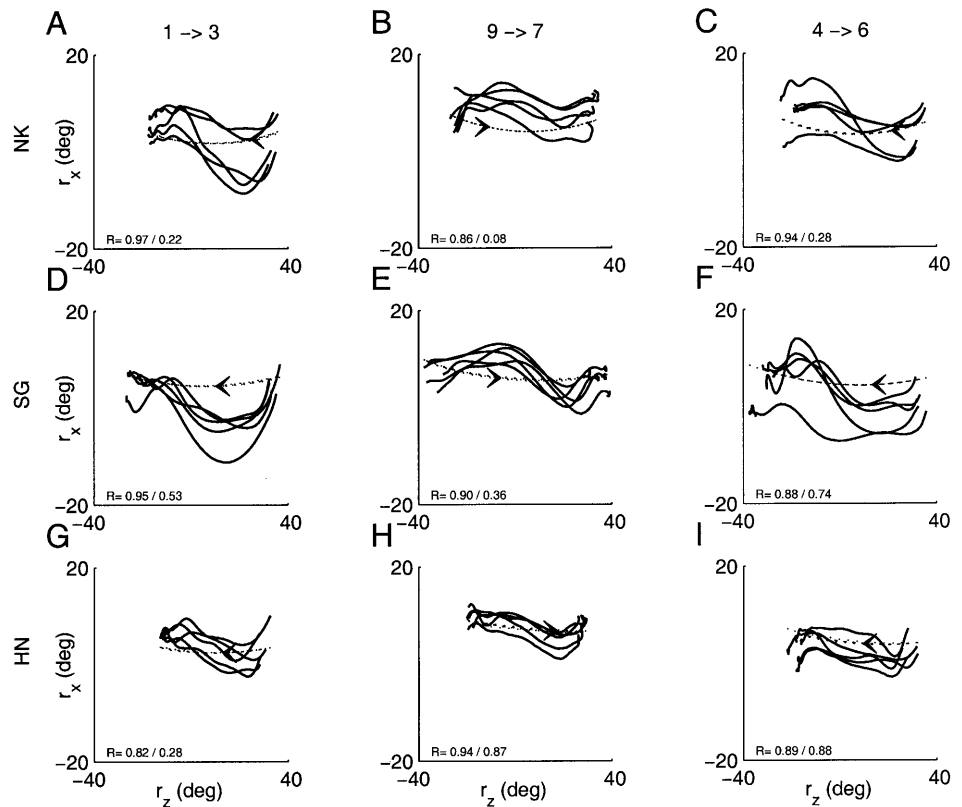
the surface does not reflect just random noise but, instead, reveals stereotyped differences. For example, in Fig. 3D the four solid lines show data of four horizontal arm movements from target 1 (upper-left) to target 3 (upper-right, see Fig. 2). Apart from a more or less constant offset of a few degrees in torsional (r_x) direction, the four trajectories have a very similar shape, with the r_x component (a measure for torsion of the upper arm) initially decreasing from a value close to the surface, then increasing to larger values (corresponding to maximal excursions relative to the surface of 4 to 9°) before finally returning again to a smaller value with a torsion close to the fitted surface.

The rotation vectors in Fig. 4 represent the orientations of the head, for the same subject as in Fig. 3 (subject SG). The upper panels show the rotation vectors representing the static orientations, i.e. orientations with angular velocities below $10^\circ/\text{s}$; the rotation vectors in the lower panels represent orientations with angular velocities higher than $10^\circ/\text{s}$.

Figure 4A shows a frontal view on the rotation vectors for head orientations at rest. Comparison of the static data for facing (Fig. 4A) and for pointing (Fig. 3A) reveals that there is more scatter in facing direction (Fig. 4A) than in pointing direction (Fig. 3A) for each of the targets.

Figure 4B presents the same data as Fig. 4A in side view in order to show the shape of the surface as clearly as possible. The surface fitted to the head orientations is mainly characterized by a twist coefficient (coefficient e

Fig. 5A–I Arm movement trajectories for three pairs of initial and final targets for three subjects. *Thick lines* represent the five trajectories with a high velocity for movements from target 1 to 3 (**A, D** and **G**), from target 9 to 7 (**B, E** and **H**) and for movements from target 4 to 6 (**C, F** and **I**). Trajectories are displayed for subject NK (**A–C**), subject SG (**D–F**) and subject HN (**G–I**). The *dotted lines* indicate the projection of the trajectory in the 2-D surface. *Arrows* indicate the direction along the trajectory in time. In each panel, the mean of the correlation coefficients between each of the trajectories and the mean of the four other trajectories (r_{mean}) as well as the mean of the correlation coefficients between the trajectories and the predicted trajectories along the surface (r_{surface}) is indicated in the lower left corner: R as $r_{\text{mean}}/r_{\text{surface}}$



in Eq. 1; see e.g. Medendorp et al. 1999; Ceylan et al. 2000). Although the amount of twist varies between subjects (mean twist coefficient -0.62 , SD 0.23 , range -0.35 to -0.88), the twist coefficient is very prominent for all subjects. The shape of the surface for the head is therefore very similar for all subjects. The large twist coefficient indicates that the shape of the surface fitted to the head data differs from the shape of the surface fitted to the arm data, which has a much smaller twist coefficient.

The standard deviation of the head data relative to the surface for subject SG in Figs. 4A, B is 1.8° , which is clearly smaller than the standard deviation relative to the surface fitted to the arm data (3.1°) for the same subject shown in Figs. 3A, B. For all subjects, the mean scatter of the head data relative to the surface was 2.6° (SD 0.5° , range 1.8 to 3.2°). The standard deviation relative to the surface is significantly smaller for head data than for arm data with mean values of 2.6 and 3.8° , respectively [$F(1,8)=11.8$, $P<0.025$].

Figure 4C shows the same static data for the head as shown in Figs. 4A, B, complemented with the rotation vectors for head orientations during the movements that were made at self-paced velocities. For all subjects, the scatter of the rotation vectors of the orientations during movement relative to the surface was larger than that of the static data (for the subject SG, 2.3° vs 1.8°). A t -test showed that this difference in scatter was significant ($t=5.36$, $P<0.05$).

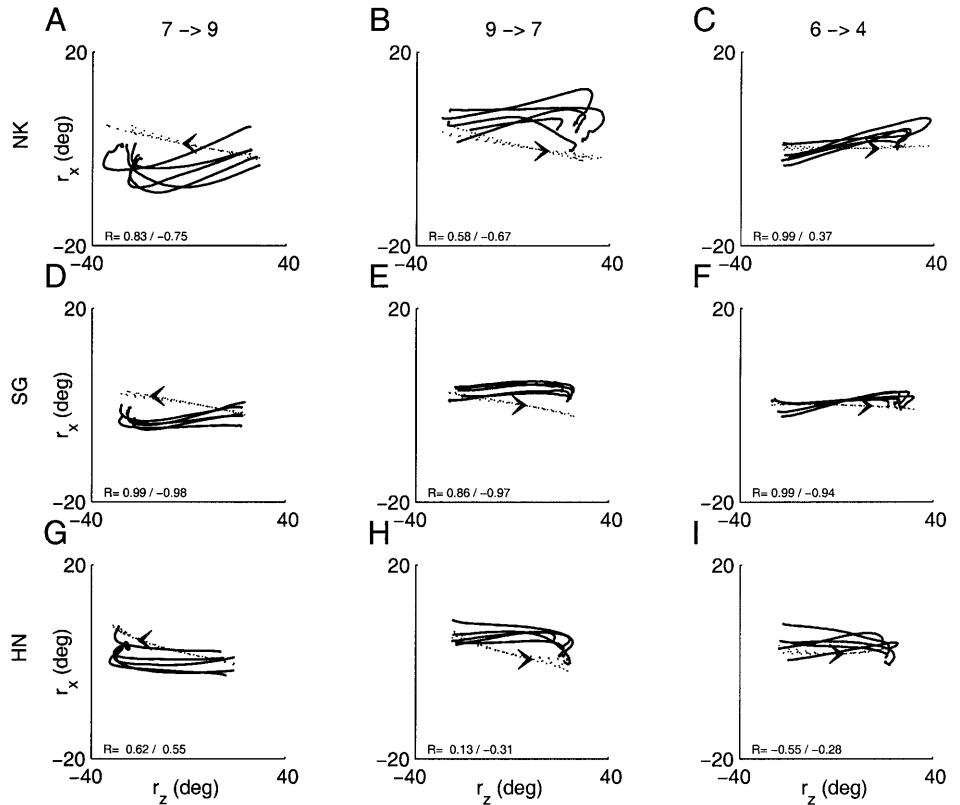
As with the arm data, a more detailed analysis of the head data demonstrates that the scatter of the rotation

vectors relative to the surface reveals stereotyped differences. Figure 4D shows four head trajectories from target 9 to target 7 (lower-right and lower-left, respectively, see Fig. 2). All four trajectories are very similar. The rotation vectors follow a more or less straight trajectory from the starting orientation close to the surface and, in the final phase of the movement, bend towards the end orientation close to the surface. The trajectories in Fig. 4D deviate from the surface with maximal excursions of 2 to 4° .

The data in Figs. 3D and 4D illustrate that trajectories of rotation vectors for movements with the same initial and final orientation tend to deviate from the curved surface fitted to the static rotation vectors in a consistent, reproducible way. Although the orientations at the beginning and end of a movement reveal a random scatter relative to the fitted surface, the orientations during a movement reveal consistent and reproducible deviations relative to the surface. The fact that the trajectories of rotation vectors revealed consistent deviations from the surface was found for many target pairs, although the shape of the deviations was different for movements between different target pairs. This is illustrated in more detail in Figs. 5 and 7 for the arm and in Fig. 6 for the head.

Figure 5 shows a further analysis of the trajectories of rotation vectors during high-velocity arm movements (see Materials and methods) for three target pairs (columns) for three subjects (rows). Figures 5A–C show 2-D projections in the r_x - r_z plane of rotation vectors

Fig. 6A–I Head movement trajectories for three pairs of initial and final targets, for three subjects. *Thick lines* represent five trajectories with a high velocity for movements from target 7 to 9 (A, D and G), from target 9 to 7 (panels B, E and H) and for movements from target 6 to 4 (C, F and I). Trajectories are displayed for subject NK (A–C), subject SG (D–F) and subject HN (G–I). The *dotted lines* indicate the projection of the trajectory in the 2-D surface. Arrows indicate the direction along the trajectory in time. The mean of the correlation coefficients between each of the trajectories and the mean of the four other trajectories (r_{mean}) as well as the mean of the correlation coefficients between the trajectories and the predicted trajectories along the surface (r_{surface}) is indicated in the lower left corner of each panel: R as $r_{\text{mean}}/r_{\text{surface}}$



obtained from subject NK. Movement paths displayed in Fig. 5A represent rotation vectors of five movements from target 1 to target 3. To illustrate the differences between the movement data and the static data in the curved surface, dotted lines represent the projection of these movement trajectories on the curved surface (see Materials and methods). Since the projections of the different movements almost fully overlap, the five dotted lines can hardly be distinguished. Apart from a more or less constant offset relative to the surface, the trajectories of rotation vectors for the arm are very similar.

Comparison of trajectories between the same pair of targets for different subjects reveals clear similarities between the trajectories. For example, Figs. 5A, D and G show rotation vectors for movements from target 1 to target 3 for subjects NK, SG and HN, respectively. Trajectories start with a positive r_z component and move towards a negative r_z component (movement direction is indicated by an arrow). For the movement from target 1 to target 3, all subjects showed an initial decrease in torsion (r_x component) larger than that predicted by the surface and, thus, the trajectories deviate from the surface. This decrease is followed by an increase in torsion and a final decrease in torsion leads the trajectory back to the surface. Similar observations can be made for movements from target 9 to target 7 (Figs. 5B, E and H) and for movements from target 4 to target 6 (Figs. 5C, F and I).

Figure 6 shows the rotation vectors for head movements between three pairs of targets for three subjects.

Just as for the arm, trajectories between the same target pairs are very similar, apart from a small offset relative to the surface. Figs. 6A, D and G show rotation vectors for movements from target 7 to target 9 for subjects NK, SG and HN, respectively. All subjects show trajectories that start near the surface and then follow a rather straight path with a slightly decreasing torsional (r_x) component. Movement along the surface would require a very different trajectory with an increasing torsional component, as indicated by the dotted lines that represent the torsional projections of the trajectories on the surface. At the end of the movement, the torsional component increases, returning to values corresponding to that of the surface. The trajectories displayed in Figs. 6A, D and G correspond to the time interval in which movement velocity exceeds the 10°/s threshold. Therefore, by the end of the displayed trajectory, the surface may not have been reached yet. Figures 6B, E and H show rotation vectors for movements between targets 9 and 7 for the three subjects NK, SG and HN, respectively. Here, clearly all movement paths start and end near the surface, but during the movement the paths tend to have a more positive torsion relative to the projection on the surface. Finally, Figs. 6C, F and I show data for movements starting at target 6 and ending at target 4. Again, movements start with an increase in torsion, and end with a decrease, thus returning to the surface. For all subjects, similar deviations from the surface seem to occur for movements between the same target pairs.

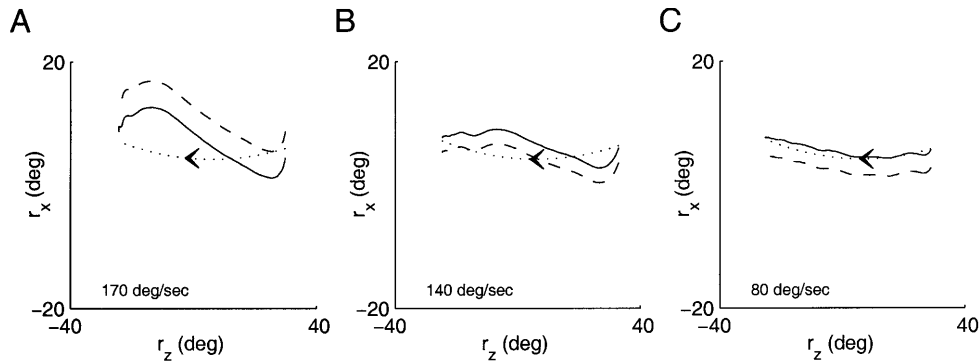


Fig. 7A–C Example of the effect of velocity on the deviation from the surface during movements of the arm, showing trajectories with peak velocities of 170°/s (**A**), 140°/s (**B**) and 80°/s (**C**). *Dashed lines* represent the original trajectories from target 7 to 9 for subject NK. *Thick lines* represent trajectories that are shifted towards the surface in torsional direction (see Materials and methods). The *dotted line* represents the projection of the trajectories on surface. *Arrows* indicate the direction along the path in time

In order to quantify the similarity between the trajectories, we compared the trajectories of the five fastest movements for each pair of targets for each subject. For each of these five movements, we compared the trajectory with the mean of the four other trajectories, by computing the correlation coefficient. We also computed the correlation coefficient between the trajectory and the predicted trajectory along the surface. Finally, for each pair of targets and for each subject, we determined the mean correlation coefficient for the comparison with the other trajectories and the mean correlation for the comparison with the predicted trajectory along the surface (see Materials and methods). This resulted in two sets of 60 correlation coefficients (12 pairs of targets for 5 subjects). In Figs. 5 and 6, the values of the mean correlation coefficients are indicated for each of the movements displayed.

For 25 of 60 correlation coefficients for arm movements, the correlation with the other trajectories was significantly higher than that with the predicted trajectory. None of the correlation coefficients with the predicted trajectory was significantly higher than that with the other trajectories.

A similar approach was followed for the trajectories of head movements. For 14 of 60 coefficients, the correlation with the mean of the other trajectories was significantly higher than that with the predicted trajectories. The correlation coefficient between the trajectories and the predicted trajectories was never significantly higher than that with the mean of the other trajectories. These results demonstrate that trajectories during a movement are often very similar. They are closer to each other than to the predicted trajectory in the 2-D surface with rotation vectors for the arm or head at rest.

In order to investigate the effect of movement velocity on the trajectory of rotation vectors during the movement, Fig. 7 shows three trajectories obtained from subject NK, for arm movements from target 7 to target 9, for

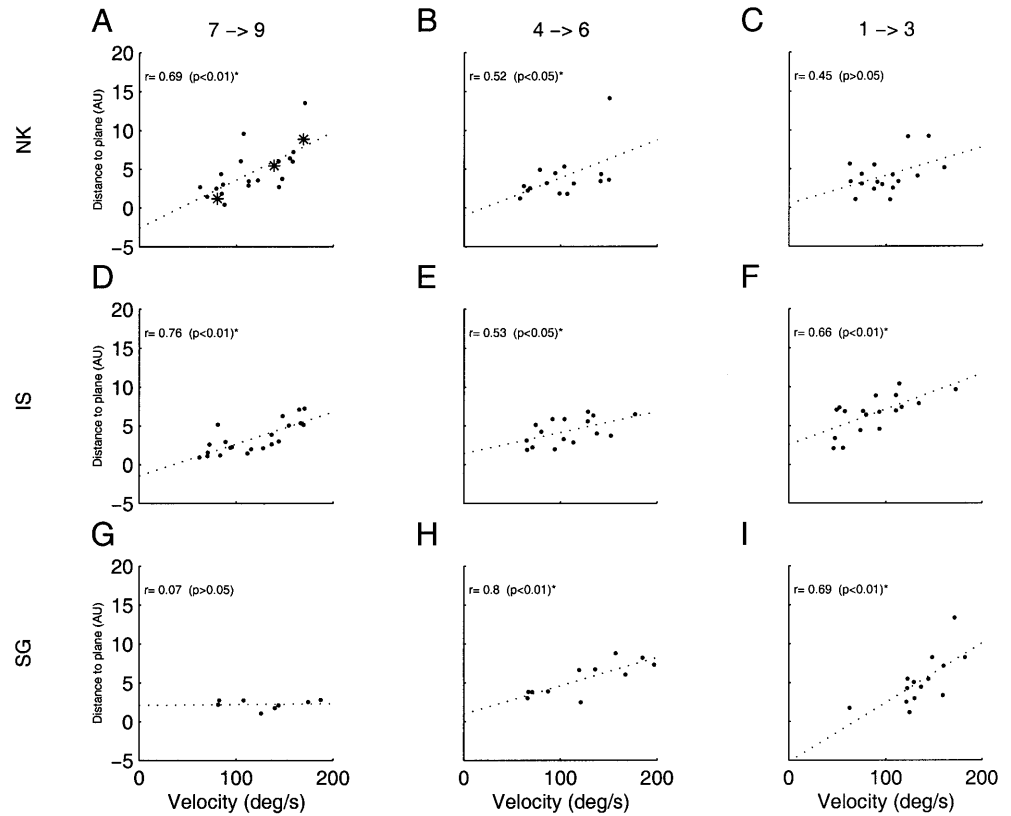
three different movement velocities. Figures 7A, B and C show movements with a peak velocity of 170, 140 and 80°/s, respectively. In order to focus on the shape of the trajectories during the movements, we corrected for the constant torsional offset as much as possible by shifting the trajectories towards the surface such that the distance of the rotation vectors towards the fitted surface is minimal at the beginning and end of the movement (see Materials and methods). After the shift, all trajectories start and end near each other.

Comparison of the trajectories in the three panels shows that for these movements the amount of deviation from the surface increases with increasing movement velocity. This was a frequently observed tendency, which will be elaborated in more detail below. Furthermore, the scatter relative to the surface varied, depending on the velocity of the movement. When only orientations at high velocities were taken into account, the scatter relative to the surface was larger than when orientations at low velocities were included.

For a quantitative evaluation of the effect of velocity on the amount of deviation, we expressed the amount of deviation in terms of the distance towards the surface integrated along the spatially resampled movement path (see Materials and methods). Figure 8 shows this measure of deviation as a function of peak angular velocity for the upper arm. Figure 8A shows all movements from target 7 to target 9 for subject NK. The data in Fig. 8A that correspond to the trajectories displayed in Fig. 7 are marked by an asterisk. Fig. 8A clearly shows a positive correlation ($r=0.69$) between peak angular velocity and the amount of deviation from the surface for these arm movements. This correlation is highly significant ($P<0.005$). An analysis of all data (12 target pairs for 5 subjects) revealed similar positive and significant ($P<0.05$) correlations for 31 of the 60 sets of arm movements. Twelve of these sets of movements showed even higher correlations, ranging from 0.68 to 0.87 ($P<0.005$). Figs. 8B, C show movements for the same subject, between targets 4 and 6 and targets 1 and 3, respectively. The middle panels (Figs. 8D–F) show the same data for movements for subject IS and the bottom panels (Figs. 8G–I) show the data for subject SG. An asterisk indicates the correlation coefficients for the data in Fig. 8 that are significant at a 5% significance level.

For head movements, we found that the correlation between peak angular velocity and the amount of deviation

Fig. 8A–I Velocity-dependent deviations from the surface for the arm for three pairs of beginning and end targets for three subjects. *Dotted lines* represent the best linear fit to the data. The corresponding correlation coefficient and its significance is displayed in each panel. **A** Data from subject NK, for movement from target 7 to target 9. *Asterisks* indicate the data for the trajectories from Fig. 7. **B, C** Data from subject NK for movements from target 4 to 6 and from target 1 to 3, respectively. **D–F** Data for subject IS; **G–I** data for subject SG



tion from the surface was less obvious than it was for arm movements. Further analysis of the head movements revealed that only 10 of 60 sets of movements had significant correlation coefficients ($P < 0.05$) between peak angular velocity and the amount of deviation from the surface. Although a frequency of 10 out of 60 movement sets is well above chance level, it is significantly smaller than that for the arm. For the head movements with a significant correlation, the dependence of the amount of deviation on peak angular velocity was about four times smaller than that for arm movements. Moreover, for head movements, both positive and negative correlations were found. This means that increasing the angular velocity leads to larger deviations for movements between some target pairs, but to smaller deviations for movements between other target pairs.

Discussion

In this study we tested whether arm and head orientations are the same during movement and at rest for identical pointing directions. Corroborating previous findings (Glenn and Vilis 1992; Hore et al. 1992; Miller et al. 1992; Theeuwes et al. 1993; Crawford et al. 1999; Medendorp et al. 1999, 2000), we found that the rotation vectors representing orientations of the upper arm and head during movements are close to a curved surface representing arm or head orientations at rest, respectively. A detailed analysis revealed that the differences between

the dynamic and static orientations were often systematic and reproducible for each target pair. This result implies a violation of Donders' law for head and upper arm movements and suggests a rejection of the movement strategy illustrated in Fig. 1A. For arm movements, the movement trajectories clearly do not correspond to fixed-axis rotations (see Fig. 5), which rejects the fixed-axis rotation strategy as illustrated in Fig. 1B. Orientations of the head during the first part of the movement follow straight trajectories in rotation vector space, which could be interpreted as evidence for a fixed-axis rotation strategy (see also Tweed and Vilis 1992; Crawford et al. 1999). The curved path at the end of the movement should then be interpreted as a correction to bring the orientations back to the 2-D surface. However, a strict interpretation of these results also rejects the strategy as illustrated in Fig. 1B for the head. The broad repertoire of alternatives, which belongs to the movement strategy of Fig. 1C, will be discussed later in the Section 'Implications for models on motor control'.

Furthermore, the differences between arm orientations during movement and at rest often become larger for higher peak velocities. A similar result was found by Nishikawa et al. (1999), who evaluated the arm plane angle (a parameter related to upper arm torsion) and reported a 'dynamic overshoot' in the change of the arm plane angle for the fastest movements in their study. For head movements, the correlation between peak velocity and difference between orientations during movement and at rest was less clear; the number of significant cor-

relations was smaller and, moreover, both negative and positive correlations were found.

Our conclusion, that the orientation of the head and arm during movements is different from that at rest, may seem contradictory to previous observations, which did not report any differences between orientations of the arm and head during movements and at rest (Glenn and Vilis 1992; Hore et al. 1992; Miller et al. 1992; Theeuwens et al. 1993; Medendorp et al. 1999). However, this apparent contradiction can be resolved easily. Our data are similar to that in the previously mentioned studies. Based on the fact that the scatter relative to the surface was almost the same in both conditions, these studies concluded that Donders' law was obeyed in static *and* dynamic conditions. In agreement with these studies, the present study showed that the size of the scatter is roughly the same in static and dynamic conditions. The slightly larger scatter in the dynamic condition in this study may be related to the higher movement velocities used relative to that used in previous studies, which only tested self-paced velocity movements (e.g. Hore et al. 1992; Miller et al. 1992; Theeuwens et al. 1993; Medendorp et al. 1999). However, in addition to the results of previous studies, the results of this study show that orientations of the head and upper arm do not scatter randomly during movements between a given target pair but vary in a systematic and consistent way across and within subjects. These results imply a violation of Donders' law, which was not concluded by previous authors.

Furthermore, the controversy in the literature as to whether Donders' law is valid for static upper arm orientations (see Soechting et al. 1995; Gielen et al. 1997) may raise the question of whether the use of a 2-D surface, fitted to the orientations at rest, as a reference to evaluate orientations during movements is a valid procedure. The 2-D surface is a least-squares fit, which minimizes the variance of the data relative to the fitted surface. Consequently, it is the best description of the data at rest and can therefore be used as a reference. Figure 3C shows that orientations during a movement follow reproducible trajectories in rotation vector space and that these trajectories do not scatter randomly. Therefore, the conclusion that orientations during movement differ from orientations at rest is independent of the interpretation of the fitted 2-D surface and, consequently, is not affected by any controversy about the validity of Donders' law for orientations at rest.

Orientations during a movement were found to have a small torsional bias of 2 or 4° at most, for the head or arm, respectively, values which remain approximately constant throughout the movement (see Figs. 5 and 6). In order to compare the shape of the trajectories of orientations during movements at different velocities, we had to correct for this bias (see Fig. 7). Support for this procedure to correct for the torsional bias without affecting the shape of the trajectory is provided by Hore et al. (1992), who instructed subjects to start arm movements with a torsional offset and found that this offset remained constant throughout the movement.

Both for the arm and for the head, the movement trajectories show reproducible deviations from the surface that describes orientations at rest. Although the shapes of these deviations are very similar for different movement velocities, the amplitudes of the deviations differ depending on movement velocity. For half of the target pairs, the observation that differences between orientations during movement and at rest become larger for higher peak velocities was significant. For head movements, the effect of peak velocity on the difference between orientation during movement and at rest was significant for a much smaller proportion (about 16%) of the movements. The correlation was relatively small and not as clear as for the arm; for some targets, peak velocity and head movements revealed a negative correlation, whereas for other targets a positive correlation was found. At this moment, we cannot provide a satisfying explanation for the different effects of peak velocity on the orientations during movements for the arm and head.

Implications for models on motor control

Previous studies on arm and head movements have mainly focused on the orientation of the arm or head at the end of a movement. In the present study, we focused on the orientations during movement and compared them with orientations at rest. One of the main results of this study is that dynamic orientations of the upper arm and head differ from static orientations for the same pointing or facing direction. This raises the question of whether differences between static and dynamic orientations are the result of a neural strategy or whether these deviations are just small artefacts due to inaccuracies in motor programming by the CNS. This issue will be addressed in the following sections.

Models for arm movements

As explained in the Introduction, there is abundant evidence that final orientation after a reaching movement is planned in advance and that it is used by the CNS in motor programming. This is in agreement with the observation that orientations at the beginning and end of movements are well described by a 2-D surface, and with the observation that orientations at the end of a movement do not depend on movement velocity (Nishikawa et al. 1999).

The extended arm can be modelled as a solid cylinder with the same inertia for movements in elevation and azimuth. If movements of such a cylinder are constrained by an efficiency criterion [such as predicted, for example, by the minimum work hypothesis (Soechting et al. 1995) or by minimum torque change (Uno et al. 1989)], rotations in the shoulder should be fixed-axis angular rotations with the smallest possible rotation angle. Fixed-axis rotations bring the arm to the final position by a straight trajectory in rotation vector space (similar to Fig. 1B),

which obviously is not the case (see curved trajectories of rotation vectors during movements in Figs. 3, 4, 5 and 6).

Flash (1987) proposed that the paths of the end effector for multi-joint arm movements are the result of a virtual trajectory of equilibrium points. The observed path might differ from the virtual path because of the complex biomechanical properties of the arm. If so, these differences will be more prominent for higher movement velocities. The result that deviations of arm orientations during movements relative to orientations at rest are larger for higher movement velocities could therefore be considered compatible with this model. However, we will argue that the biomechanical properties of the arm (e.g. inertia) and gravitation cannot explain the shape of the deviations from the surface observed in this study. Our analyses demonstrate that the differences between orientations of the arm in static conditions and during movements are mainly in torsional direction. The inertia of the fully extended arm is the same for movements in elevation and azimuth. Therefore, the torsional component of the spatial paths of the upper arm should not be different from that of the virtual path for horizontal and vertical movements. Taking the effect of gravity into account might lead to deviations of the vertical component of movement paths relative to the virtual path, but does not effect the torsional component of the arm.

Another explanation for the differences in orientations at rest and during movement may arise from the neuromuscular properties of the arm. Muscles in the shoulder produce accelerations in a mixture of directions. Activation of the pectoralis major muscle, for example, produces both abduction and endorotation of the upper arm. Activation of a muscle to accelerate the arm in a specific direction will thus simultaneously introduce accelerations in unintended directions. Activation of other muscles is then needed to cancel these byproducts.

Ghez and Gordon (1987) reported that during isometric impulses and steps of flexor force in the elbow, flexor and extensor muscles are successively activated. They concluded that the neural commands to opposing muscles acting at a joint must be adapted to constraints imposed by the properties of the neuromuscular plant. Such co-activation could be triggered by reflexes. Gielen et al. (1988) have shown that long latency stretch reflexes (50–75 ms) incorporate coordinated responses from various muscles, but that short-latency reflexes do not. It is well known that latencies of mono-synaptic reflexes are different for various muscles in the human arm (Lacquaniti and Soechting 1986; Soechting and Lacquaniti 1988). These differences in latency have been attributed to differences in conduction time along nerve fibres from motoneurons in the spinal cord to the muscle. These differences will have a small effect on the precise coordination of movements in 3-D for low movement velocities. For fast movements, however, the effect of differences in activation time for co-activated muscles on the movement trajectories will become more prominent. This might explain the correlation between peak

velocity on the one hand, and the difference between orientations during movement and those at rest on the other hand.

Models for head movements

Tweed (1997) postulated a model for eye-head saccades in 3-D, which assumes that orientations of the head are determined by a system (Donders' operator) that specifies head orientations according to Donders' law, followed by a system (so-called head-pulse generator) that generates the proper motor commands to move the head towards the final orientation (see also Medendorp et al. 1999). Deviations during movement could be due to the fact that the Donders' operator is located before the pulse-generator. From this point of view, the fact that the first and major part of the trajectory for head movements reported in this study is a more or less straight path in rotation vector space might indicate that the head-pulse generator induces a fixed-axis rotation for the head, followed by a correction movement, which brings the end of the trajectory back to the surface that characterizes the static data.

If arm movements are described by a similar model, the equivalent of the head-pulse generator for the arm might, in a similar way, be located after the Donders' generator, which may lead to violations from Donders' law during movement. This is compatible with previously proposed models for arm movements that postulate internal models that mimic the input/output characteristics, or their inverse, of the motor apparatus to move the limb from the starting to the (predefined) final orientation (see Kawato 1999). According to this line of thought, the trajectories would be the result of a deliberate planning by the CNS, instead of a distortion of some planned trajectory.

For each pair of targets the very reproducible trajectories can have different torsional offsets of at most 2 or 4° for the head and arm, respectively, which remain approximately constant throughout the movement. This suggests that the arm or head constraints are not implemented at the level of position commands but presumably at the level of velocity commands or maybe at some higher level such as acceleration (Ceylan et al. 2000; Medendorp et al. 2000). These so-called non-holonomic constraints do not restrict the allowable positions of the system, but only the permitted velocities in certain positions. Moreover, while velocity-level control can account for the fact that head and arm depart from their static Donders' surface during movements, position-level control would force one to conclude that the Donders' operator is outside of the motor feedback loop.

In order to discriminate between the various models, more detailed studies on postures during movements are necessary. This study provides a first step towards these studies by presenting a new framework to analyse orientations during movements in great detail.

References

- Ceylan MZ, Henriques DYP, Tweed DB, Crawford JD (2000) Task-dependent constraints in motor control: pinhole goggles make the head move like an eye. *J Neurosci* 20:2719–2730
- Crawford JD, Ceylan MZ, Klier EM, Guitton D (1999) Three-dimensional eye-head coordination during gaze saccades in the primate. *J Neurophysiol* 81:1760–1782
- Flanders M, Helms-Tillery SI, Soechting JF (1992) Early stages in sensori-motor transformations. *Behav Brain Sci* 15:309–362
- Flash T (1987) The control of hand equilibrium trajectories in multi-joint arm movements. *Biol Cybern* 57:257–274
- Ghez C, Gordon J (1987) Trajectory control in targeted force impulses. *Exp Brain Res* 67:225–240
- Gielen CCAM, Ramaekers L, Van Zuylen EJ (1988) Long-latency stretch reflexes as co-ordinated functional responses in man. *J Physiol* 407:275–292
- Gielen CCAM, Vrijenhoek EJ, Flash T, Neggers SFW (1997) Arm position constraints during pointing and reaching in 3-D space. *J Neurophysiol* 78:660–673
- Glenn B, Vilis T (1992) Violations of Listing's law after large eye and head gaze shifts. *J Neurophysiol* 68:309–318
- Gréa H, Desmurget M, Prablanc C (2000) Postural invariance in three-dimensional reaching and grasping movements. *Exp Brain Res* 134:155–162
- Haustein W (1989) Considerations on Listing's Law and the primary position by means of a matrix description of eye position control. *Biol Cybern* 60:411–420
- Hore J, Watts S, Vilis T (1992) Constraints on arm position when pointing in three dimensions: Donders' law and the Fick gimbal strategy. *J Neurophysiol* 68:374–383
- Kawato M (1999) Internal models for motor control and trajectory planning. *Curr Opin Neurobiol* 9:718–727
- Lacquaniti F, Soechting JF (1986) responses of mono- and bi-articular muscles to load perturbations of the human arm. *Exp Brain Res* 65:135–144
- Medendorp WP, Melis BJM, Gielen CCAM, Van Gisbergen JAM (1998) Off-centric rotation axes in natural head movements: implications for vestibular reafference and kinematic redundancy. *J Neurophysiol* 79:2025–2039
- Medendorp WP, Van Gisbergen JAM, Horstink MWIM, Gielen CCAM (1999) Donders' law in torticollis. *J Neurophysiol* 82:2833–2838
- Medendorp WP, Crawford JD, Henriques DYP, Van Gisbergen JAM, Gielen CCAM (2000) Kinematic strategies for upper arm-forearm coordination in three dimensions. *J Neurophysiol* 84:2302–2316
- Miller LE, Theeuwes M, Gielen CCAM (1992) The control of arm pointing movements in three dimensions. *Exp Brain Res* 90:415–426
- Nishikawa KC, Murray ST, Flanders M (1999) Do arm postures vary with the speed of reaching? *J Neurophysiol* 81:2582–2586
- Radau P, Tweed D, Vilis T (1994) Three-dimensional eye, head and chest orientations after large gaze shifts and the underlying neural strategies. *J Neurophysiol* 72:2840–2852
- Rosenbaum DA, Loukopoulos LD, Meulenbroek RGJ, Vaughan J, Engelbrecht SE (1995) Planning reaches by evaluating stored postures. *Psychol Rev* 102:28–67
- Soechting JF, Lacquaniti F (1988) Quantitative evaluation of the electromyographic responses to multidirectional lean perturbations of the human arm. *J Neurophysiol* 59:1296–1313
- Soechting JF, Buneo CA, Herrmann U, Flanders M (1995) Moving effortlessly in three dimensions: does Donders' law apply to arm movement? *J Neurosci* 15:6271–6280
- Straumann D, Haslwanter Th, Hepp-Reymond MC, Hepp K (1991) Listing's law for eye, head and arm movements and their synergistic control. *Exp Brain Res* 86:209–215
- Theeuwes M, Miller LE, Gielen CCAM (1993) Are the orientations of head and arm related during pointing movements? *J Mot Behav* 25:242–250
- Tweed D (1997) Three-dimensional model of the human eye-head saccadic system. *J Neurophysiol* 77:654–666
- Tweed D, Vilis T (1992) Listing's law for gaze directing head movements. In: Berthoz A, Vidal PP, Graf W (eds) *The head-neck sensory-motor system*. Oxford University Press, New York, pp 387–391
- Uno Y, Kawato M, Suzuki R (1989) Formation and control of optimal trajectory in human multi-joint arm movement. Minimum torque-change model. *Biol Cybern* 61:89–101
- Veldpaus FE, Woltring HJ, Dortmans LJM (1988) A least-squares algorithm for the equiform transformation from spatial marker co-ordinates. *J Biomech* 21:45–54